

## Arsenic Removal by Nanoscale Magnetite in Guanajuato, Mexico

Jesse Walter Farrell,<sup>1,\*</sup> John Fortner,<sup>2</sup> Sarah Work,<sup>3</sup> Carolina Avendano,<sup>4</sup> Natalia I. Gonzalez-Pech,<sup>4</sup> Rafael Zárate Araiza,<sup>5</sup> Qilin Li,<sup>3</sup> Pedro J.J. Álvarez,<sup>3</sup> Vicki Colvin,<sup>4,6</sup> Amy Kan,<sup>3</sup> and Mason Tomson<sup>3</sup>

<sup>1</sup>Water Management, Schlumberger, Houston, Texas.

<sup>2</sup>Department of Energy, Environmental and Chemical Engineering, Washington University in St. Louis, St. Louis, Missouri.

<sup>3</sup>Department of Civil and Environmental Engineering, Rice University, Houston, Texas.

<sup>4</sup>Department of Chemistry, Rice University, Houston, Texas.

<sup>5</sup>CITAG, Guanajuato, Mexico.

<sup>6</sup>Department of Chemical and Biomolecular Engineering, Rice University, Houston, Texas.

Received: November 1, 2013

Accepted in revised form: April 18, 2014

### Abstract

Increasingly, cities in Latin America are recognizing the importance of drinking water quality on public health. A water assessment of Guanajuato, Mexico, and surrounding areas indicated naturally occurring arsenic in some wells above the Mexican drinking water standard of 25  $\mu\text{g/L}$  and the World Health Organization recommendation of 10  $\mu\text{g/L}$ . This initiated a collaborative effort with the city to evaluate a new arsenic removal method using high surface area magnetite sorbents. Nanoscale (20 nm) magnetite particles, previously shown to effectively adsorb arsenic in batch systems, were packed in sand columns to create a continuous treatment process. Design and operating variables were evaluated to confirm that magnetite-to-sand ratio and residence time most significantly affected arsenic breakthrough profiles. Subsequently, a pilot column with 456 g (ca. \$2.50 USD) of a commercially available, food-grade magnetite (98 nm effective particle diameter) from a pigment manufacturer demonstrated removal of the equivalent arsenic contained in 1,360 L of Guanajuato groundwater. Although pH reduction dramatically improved arsenic adsorption in batch isotherms, no improvement in arsenic removal efficiency was observed when applied to pilot-scale, field columns in Guanajuato. Interference effects (e.g., from background silica) and changes to surface species over time may impact adsorption differently in column versus batch systems. Overall, this work represents one of the first pilot studies of a nanotechnology-enabled water treatment system, and it demonstrates the potential and additional challenges for taking nanoscale magnetite or other highly researched nanomaterials into a complex full-scale setting.

**Key words:** adsorption; arsenic; breakthrough; case study; column; drinking water treatment; Guanajuato; isotherms; Mexico; nanomagnetite; nanotechnology; sand filtration

### Introduction

ARSENIC IS A SEMI-METAL that occurs naturally in the environment and as a by-product of industrial activity (Plant *et al.*, 2005). The presence of arsenic in drinking water is a widespread problem in many developing regions. Long-term exposure to arsenic can result in hyperkeratosis, skin lesions, and cancer of the bladder, lungs, kidneys, and skin. There is some evidence that elevated exposure to arsenic increases risk of Type 2 diabetes (Navas-Acien *et al.*, 2008), which is particularly concerning Mexico where diabetes may cost the Mexican government three-quarters of its total health care spending annually (Phillips and Salmeron, 1992).

City officials in Guanajuato, Mexico, provided a test-bed site for researchers with the Center for Biological and Environmental Nanotechnology (CBEN) at Rice University to develop nanomaterial-based water treatment technologies suited to address water quality needs in Guanajuato. Heavy metal contamination of their water supply was a concern due to nearby silver and gold mining activity. Arsenic concentrations as high as 33  $\mu\text{g/L}$  in Guanajuato and 266  $\mu\text{g/L}$  in surrounding towns were observed from municipal groundwater wells. In response to these findings, Guanajuato officials agreed to support a field trial of a nanomagnetite-based filter capable of removing arsenic from their groundwater.

This work represents one of the first case studies to evaluate a nanotechnology-enabled conventional treatment process for water supply in a developing country. We demonstrate under real-world conditions that augmenting sand filters with nanoscale food-grade magnetite could benefit

\*Corresponding author: Oilfield Water Management, Schlumberger, 5599 San Felipe, Houston, TX 77056. Phone: 281-285-4390; Fax: 281-285-1927; E-mail: jfarrell01@slb.com

arsenic removal, and provide data to inform design and feasibility assessment.

### Background

The city of Guanajuato, Mexico (population ca. 150,000) is the capital of the state of Guanajuato (Supplementary Fig. S1). Local industry is primarily driven by silver and gold mining, oil production, clothing manufacturing, and tourism. Because of its historical importance as the world's leading silver mining center in the 18th century and overall high level of preservation, the city of Guanajuato has been designated a UNESCO World Heritage site.

Before construction of their first dam in 1749, Guanajuato residents primarily relied on surface (river) water. However, during extremely dry seasons the river bed would go dry and residents resorted to drinking water from deep mines, which resulted in many fatalities (Simapag, 2009). The first dam provided sufficient water supply year round and, 100 years later, was connected to 12 distribution fountains in the city. Water delivery by local "aguadores" further improved the community's access to water (Supplementary Fig. S2). In 1880, an additional dam was built called La Esperanza, meaning "The Hope" in Spanish, which provided adequate supply to allow for direct plumbing to homes year round (Supplementary Fig. S3). The dams supplied untreated river water to city homes until the first water treatment plant was built in 1954. In 1983, deep groundwater wells were drilled to supplement the water supply of the growing city. By 2009, over one-half of the municipal water was supplied by the groundwater wells, some containing arsenic concentrations near the Mexican contaminant limit of 25 µg/L.

Although arsenic is found in the environment as several different species, the inorganic forms are predominant. Arsenic is usually present in drinking water sources as As(V) (arsenate,  $\text{AsO}_4^{3-}$ ) and As(III) (arsenite,  $\text{AsO}_3^{3-}$ ). The acid-base chemistry of arsenite and arsenate is such that in most natural waters As(V) is anionic ( $\text{H}_2\text{AsO}_4^-$  or  $\text{HAsO}_4^{2-}$ ) and As(III) is neutral ( $\text{H}_3\text{AsO}_3^0$ ). Efficient treatment of arsenic in drinking waters has been demonstrated with a handful of technologies as detailed by Wang and Chen (2011), and include anion exchange [primarily for As(V)], reverse osmosis, and adsorptive media. Further, adsorbents such as goethite, hematite, magnetite, zero valent iron, granular ferric hydroxide, activated alumina, aluminum oxides, titanium dioxide, iron coated sand, polymer supported metals, and surface modified activated carbon have been demonstrated as effective adsorbents for arsenic (Hingston *et al.*, 1971; Anderson *et al.*, 1976; Gupta and Chen, 1978; Huang and Fu, 1984; Raven *et al.*, 1998; Arai *et al.*, 2002; Dixit and Hering, 2003; Mohan and Pittman, 2007; Hristovski *et al.*, 2009; Mamindy-

Pajany *et al.*, 2011; Wang and Chen, 2011). Given that these adsorbents come in various shapes and sizes and their adsorption kinetics and equilibrium capacities are affected by many interrelated solution conditions (e.g., pH, ionic strength, arsenic concentration, concentrations of competing ions, speciation of arsenic, redox potential, and temperature), the published literature on these arsenic adsorbents is vast.

While most adsorbents show preference toward the less toxic As(V), nanoscale magnetite is one iron oxide-based material that not only demonstrates high sorption capacity, but can adsorb As(III) and As(V) with similar affinity (Chowdhury *et al.*, 2001; Yavuz *et al.*, 2006; Gimenez *et al.*, 2007; Jonsson and Sherman, 2008; Shipley *et al.*, 2009; Bujnakova *et al.*, 2013). In general, the adsorption capacity of these and other materials is related to favorable surface enthalpies of interaction and available surface area, which is inversely related to particle diameter. Interestingly, though, at particle diameters below 20 nm, nanomagnetite has been found to adsorb a proportionally greater amount of arsenic than would be projected from its larger, micron-sized counterpart (Mayo *et al.*, 2007). In addition, nanoscale magnetite (magnetite is the most magnetic naturally occurring mineral) has generated interest due to its superparamagnetic properties, which underpin the potential for low energy, high efficiency separations and removal/capture by low magnetic fields (Yavuz *et al.*, 2006). Lastly, food-grade nanoscale magnetite is now available in bulk quantities at a cost that is competitive with other adsorbents discussed—especially, when considering the potential for material regeneration and reuse.

When packed into sand columns, adsorbents can be immobilized and allow the filter media to efficiently remove contaminants due to rapid adsorption kinetics (Hristovski *et al.*, 2007). Columns or sand beds can be operated economically as point-of-use or larger treatment systems as they require little capital infrastructure or technical expertise. In this work nanoscale magnetite, with the benefit of its high adsorption capacity and its similar affinity for both As(III) and As(V), was selected to be incorporated into sand columns to remove arsenic from Guanajuato groundwater. In addition, the magnetic properties of magnetite can be taken advantage of, even in a column setting, by allowing efficient magnetic separation of any magnetite fines that might migrate from the column during operation or regeneration.

### Experimental Protocols

#### Materials

Groundwater samples were collected from Guanajuato municipal well No. 8 and from the Evangeline aquifer (1,600

TABLE 1. COMPOSITION OF EVANGELINE (EVG) AND GUANAJUATO (GTO) GROUNDWATERS BEFORE ADJUSTMENT OF pH AND SPIKED WITH ARSENIC FOR ADSORPTION ISOTHERMS

	pH	Cond	Alkalinity	Na	Ca	Mg	Fe	PO <sub>4</sub>	SiO <sub>2</sub>	As	U	V	Zn
	SU	µS/cm	mg/L as CaCO <sub>3</sub>	mg/L	mg/L	mg/L	mg/L	mg/L	mg/L	µg/L	µg/L	µg/L	µg/L
Evg GW	8.2	558	208	104	11.2	3.0	0.2	0.08	18.5	2.1	0.1	0.0	4.7
Gto GW	8.3	510	144	122	3.5	0.2	0.4	0.12	48.1	9.1	3.1	4.4	5.5

ft depth) for comparison (analyses displayed in Table 1). A selection of magnetite particles was evaluated from a variety of commercial sources. However, only three materials are included: (1) the product with the highest adsorption capacity (20 nm magnetite; Reade Advanced Materials), (2) the product with the lowest adsorption capacity ( $<5\ \mu\text{m}$  magnetite powder; Sigma-Aldrich), and (3) the product with food-grade certification that was most economical per mass of arsenic adsorbed for use in larger-scale pilot columns (98 nm magnetite, 78P; Rockwood Pigments). Column studies were conducted with 20 and 98 nm magnetite products, pictured in Figure 1 alongside photographs of the bench-scale and pilot-scale columns. The surface area of each product was determined by Brunauer-Emmett-Teller (BET) analysis of a known mass of that product to calculate the given “effective” particle diameter, defined here as the particle diameter of an equivalent mass of uniformly sized, spherical particles. There was significantly wider distribution in particle size for the Rockwood Pigments nanomagnetite than for the Reade nanomagnetite. A sieve analysis (not shown) confirmed that particles of both products were in aggregated state with a mass-weighted average size of about  $100\ \mu\text{m}$ . Sea-sand (pre-washed from Fisher Scientific) was used as a support media for both mixing with magnetite and providing containment above and below the magnetite/sand mixture. Stock solution of As(V) ( $50\ \text{mg/L}$ ) was prepared by dissolving  $\text{As}_2\text{O}_5 \cdot 3\text{H}_2\text{O}$  (Sigma-Aldrich) into  $18.2\ \text{M}\Omega/\text{cm}$  Milli-Q water and was used to spike groundwater for laboratory experiments. For adsorption isotherms and bench-scale columns, concentrated trace-metal grade  $\text{HNO}_3$  (Fisher Scientific) or  $1\ \text{M}$  NaOH (Fisher Scientific) was used for pH adjustment of groundwater. For pilot-scale columns, trace metal grade  $\text{HNO}_3$  (Fisher Scientific) or Certified ACS Plus Glacial Acetic Acid (Fisher Scientific) were used.

#### Batch adsorption isotherms

Adsorption isotherms were conducted at room temperature and under open atmospheric conditions with Evangeline or Guanajuato groundwater spiked to  $75\ \mu\text{g/L}$  with As(V). The pH was left as-is or was adjusted to 5.5, 6.5, or 7.5. For each isotherm experiment, a series of masses (0, 4, 8, 17.5, 32.5,

and 65 mg) were weighed into 60 mL vials (Environmental Express). The given groundwater solutions were added gravimetrically to 50 g and vials were mixed end-over-end at 3 rpm for 24 h. Afterward, a 0.62 T neodymium magnet (K&J Magnetics, Inc.) was placed below to facilitate rapid particle separation. The supernatant was then filtered with a  $0.45\ \mu\text{m}$  polyethersulfone (PES) syringe filter (Whatman) and preserved with trace-metal grade acid and analyzed by inductively coupled plasma-optical emission spectrometer (ICP-OES) and inductively coupled plasma-mass spectrometer (ICP-MS), as described later. The arsenic adsorbed was calculated as that removed from solution. A control blank replicates containing no magnetite were run with each set of experiments to account for any other losses, which were negligible.  $K_d$  values were determined based the calculation of arsenic adsorbed and the measured mass of magnetite in each vial.

One batch adsorption isotherm was conducted to simulate the Guanajuato groundwater conditions of high temperature and low oxygen content that might be encountered if treated directly from municipal well No. 8. A vacuum pump was used to remove oxygen from the As(V)-spiked Guanajuato groundwater. While sparging with argon for 30 min, the temperature of the solution was brought by hot plate to  $40^\circ\text{C}$ . Solution was transferred to an anaerobic chamber where vials were sealed with preweighed nanomagnetite and 50 mL of solution. The vials were agitated for 24 h in a hot water bath at  $40^\circ\text{C}$ . The magnetite was separated from solution and the solutions were prepared for arsenic analysis.

#### Bench-scale columns

For 5% and 20% by weight magnetite columns, 0.3 and 1.2 g of magnetite, respectively, were weighed into glass vials and mixed with sand for a total of 6 g of media for each vial. The mixture was shaken vigorously by hand for 1 min to disperse the magnetite throughout the sand. The mixture was poured directly into a 1-cm diameter borosilicate glass column (Omnifit) to fill  $\sim 5\ \text{cm}$  of height. Borosilicate glass beads (3 mm; ChemGlass), phosphoric acid-treated glass wool (Supelco), and pure sand were used to support the sand/nanomagnetite media on both ends. To wet the column, deionized water was pumped into the column in upflow mode

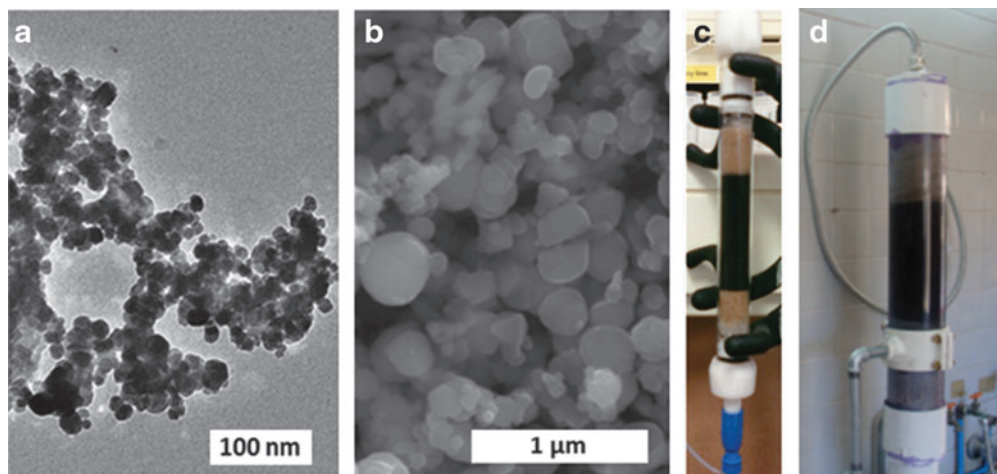


**FIG. 1.** (a) TEM of Reade magnetite, (b) SEM of Rockwood 78P magnetite, (c) 1 cm ID bench-scale column, and (d) 10.2 cm ID field-scale, pilot column. ID, internal diameter.

at 4 mL/h. The flow direction was then reversed to downflow-mode for subsequent column experiments. A Pharmacia P-500 continuous-feed, dual-syringe pump delivered feed solution to the column with < 1% variation at 3 or 34 mL/h resulting in residence times of about 36 or 3 min, respectively. During flow, black magnetite particles remained immobile except for approximately 1 cm of bleed to adjacent pure sand. Feed solution was composed of aerated Evangeline groundwater (pH 8.5) spiked to 100  $\mu\text{g/L}$  arsenic with As(V) stock solution. The feed solution was mixed by stir bar under open atmosphere. Samples of 3–10 mL were collected either by hand or by a fraction collector (Waters) on a timed interval into a 10 mL vial. Samples were then filtered with 0.45  $\mu\text{m}$  PES syringe filter, acidified to 1% by weight with concentrated trace-metal-grade  $\text{HNO}_3$ , and analyzed by ICP-OES and ICP-MS. The unit pore volume (PV) basis was taken as the pore space in the section of the column containing the sand and nanomagnetite mixture. It was calculated from the column diameter, the height of the adsorbent media section, the mass of the sand and magnetite, and the density of the sand and magnetite.

#### Pilot scale columns

For each pilot column, 10,000 L of water from Guanajuato Municipal well No. 8 was brought by truck (Supplementary Fig. S4) to a laboratory in Guanajuato where column systems were assembled as depicted in Figure 2. To prepare the feed solution for pH-adjusted experiments, first the ratio of concentrated acid (nitric or acetic acid) to groundwater was determined at the bucket-scale to obtain a pH of 5.5. Then, to facilitate dispersion and mixing, the appropriate dose of concentrated acid was diluted into a bucket of groundwater and poured into the truck gradually while being filled from the well.

In the treatment columns, the active adsorbent layer was composed of 456 g of Rockwood Pigments 78P magnetite dispersed in 2,587 g of washed sea sand, giving a magnetite to sand mass ratio of 3:17 or 15% magnetite by weight. The sand and magnetite were combined in two 2-L Nalgene, wide-

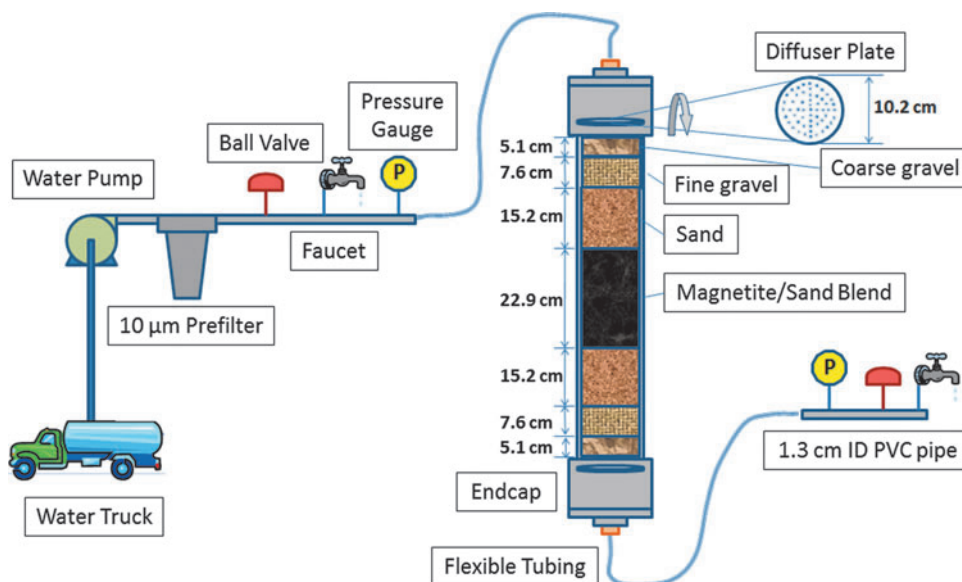
mouth containers and were vigorously shaken by hand for 5 min. Layers of washed sea sand, fine gravel, and coarse gravel were used to support and contain the media above and below the active adsorbent layer. Prior to use, fine and coarse gravel were repeatedly washed with deionized water in buckets until the wash water remained clear. Diffuser plates were machined from 0.5 cm thick Plexiglass (polymethylmethacrylate [PMMA]) sheets and perforated with 3-mm holes to permit fluid flow. Pressure-rated transparent polyvinyl chloride (PVC) pipe (0.76 m length, 10.2-cm internal diameter [ID], schedule 40) was cut to serve as the column body (Supplementary Fig. S5). Endcaps were assembled with 10.2-cm pressure-rated PVC couplings, 10.2- to 5.1-cm PVC reducers, and a 5.1- to 1.9-cm thread reducers. Adapters were used to connect to 1.9-cm flexible, metal reinforced tubing and 1.3-cm PVC line. PVC ball valves, pressure gauge dials, and metal faucet-valve sample ports were installed upstream and downstream of the columns. A 10- $\mu\text{m}$  household prefilter (US Filter) was used upstream of the column to reduce the potential for plugging by suspended solids. The PVC connections were sealed together with PVC primer and quick-set PVC cement (Harvey's Co.), while all threaded connections were lined with polytetrafluoroethylene tape to prevent leakage.

Columns were dry-packed and wetted slowly with deionized water funneled into flexible tubing connected to the bottom of the column (Supplementary Fig. S6). The funnel and tubing was lifted gradually to control the rise of fluid within the column to  $\sim 1$  cm/min (40 mL/min). Afterward, flow direction was reversed to down-flow mode to flush the column with deionized water for 1 h before running the experiment. Inlet and outlet lines were kept elevated above the column to maintain a water-lock in the column.

A flow rate of 1 L/min was established using a positive displacement pump (FMI, Inc.) or, in the case of the raw groundwater experiment, by controlling the outlet flow rate with a faucet valve. The flow rate was periodically monitored using a 500-mL graduated cylinder and adjusted as necessary.

Samples were collected by hand on a timed interval from ports before and after the column into 10 mL plastic syringes

**FIG. 2.** Schematic of pilot column setup used in Guanajuato.



and immediately passed through a 0.45- $\mu\text{m}$  PES filter (Whatman) and preserved to 1% by weight with concentrated trace-metal-grade  $\text{HNO}_3$  and refrigerated. Select unfiltered samples were collected throughout the experiment and analyzed for total iron to examine whether any breakthrough of particles occurred, but no increase in iron concentration was observed for any of the samples. The samples were packed on ice during air-transport to Rice University for analysis by ICP-MS and ICP-OES.

A portable arsenic test kit (Hach #2800000) was used to provide a real-time, semi-quantitative value for the arsenic concentration of water flowing into and out of the pilot columns in Guanajuato. The method involves reduction of arsenic to arsine gas, which was then collected on a reactive test strip and compared to a color chart (Supplementary Fig. S7). Full breakthrough was determined when the colors of the inlet and outlet water test strips were equivalent.

### Chemical analysis

The pH was measured with an Orion-Research combination glass-reference electrode in the lab and Hach platinum-series combination electrode with SensIon156 portable meter in the field, calibrated with pH 4, 7, and 10 standards (Fisher Scientific). Total alkalinity was measured by phenolphthalein and bromocresol green-methyl orange titration with sulfuric acid. Phosphate was measured by the Hach PhosVer spectrophotometric method. The Hach FerroVer method was used to measure total (particulate and dissolved) Fe. Dissolved Na, Ca, Mg, Fe, and Si were determined by Perkin Elmer Optima 4300DV ICP-OES. Dissolved Ag, As, Be, Ca, Co, Cr, Cu, Pb, Se, U, V, and Zn were determined by Perkin Elmer Elan 9000 ICP-MS analysis as described below.

Before ICP-MS measurement, a daily performance analysis and calibration was performed using 0, 0.5, 5, and 25  $\mu\text{g/L}$  standards of Ag, Al, As, Ba, Be, Bi, Ca, Cd, Co, Cr, Cs, Cu, Fe, Ga, In, K, Li, Mg, Mn, Ni, Pb, Rb, Se, Na, Sr, Tl, V, U, and Zn, diluted from a certified multi-element atomic spectroscopy standard solution from PerkinElmer. Additional certified arsenic standard (CPI International Peak Performance) and certified zinc standard (PerkinElmer) solutions were used to increase the range of these two elements to 4, 40, and 200  $\mu\text{g/L}$ . Each standard was measured in triplicate with relative standard deviations typically  $< 3\%$ , and each element gave a regression with  $R^2$  values of 0.999 or better.

### Modeling

Speciation modeling and breakthrough curve fitting were conducted in Visual Minteq (Gustafsson, 2012) and CXTFIT (Toride *et al.*, 1995), respectively.

## Results and Discussion

### Bench-scale column trials

Several design and operating parameters were tested in column trials to quantify arsenic removal by nanoparticles suspended in a sand support media. Parameters varied included the flow rate, residence time, inlet arsenic concentration, and the mass ratio of magnetite to sand. Other variations were conducted, for example, to see whether vigorously shaking the nanomagnetite aggregates with sand before loading the column would improve the breakthrough

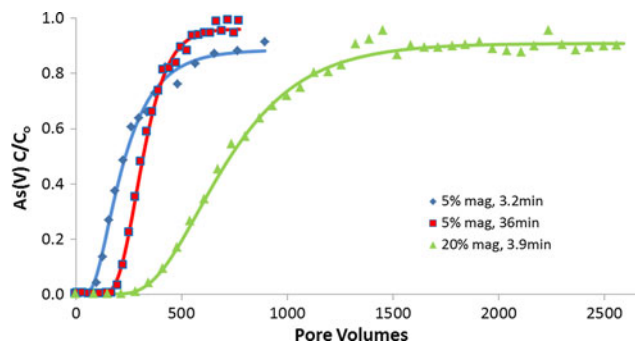


**FIG. 3.** Breakthrough of 100  $\mu\text{g/L}$  As(V)-spiked Evangeline groundwater, pH 8.5, in 1 cm diameter sand columns of 5% and 20% nanomagnetite by weight with varied residence times. Solid lines are fitted by CXTFIT.

profile by more finely dispersing the nanomagnetite, but little difference was observed. The primary factors affecting the breakthrough profile of arsenic through the column were the mass ratio of magnetite to sand in the packing media and the residence time of the solution in contact with the media (Fig. 3). The breakthrough profile is especially important for single-pass systems where the effluent arsenic must meet a specified drinking water limit. While both factors affected the breakthrough profile, residence time made little difference in the cumulative mass of arsenic retained in the column at full saturation (Fig. 4). The cumulative adsorption capacity is important for multiple-pass systems where a lead column can continue to adsorb arsenic while the effluent is passed to a lagging column to further reduce arsenic concentration below a set standard.

The most significant impact on arsenic breakthrough was observed by changing the magnetite-to-sand ratio in the packing media, as shown in Figure 3 for a feed solution of Evangeline groundwater spiked to 100  $\mu\text{g/L}$  with As(V). When the magnetite concentration within the media was increased from 5% to 20% by weight and the residence time was kept similar (3.2 and 3.9 min, respectively), the point of 50% breakthrough ( $C/C_0 = 0.5$ ) shifted from 225 PV to 712 PV. Contrary to expectation, the column containing 20% magnetite did not adsorb proportionally ( $4\times$ ) more than the column containing 5% magnetite. It adsorbed only  $3.2\times$  more. The deviation from exact proportionality may be

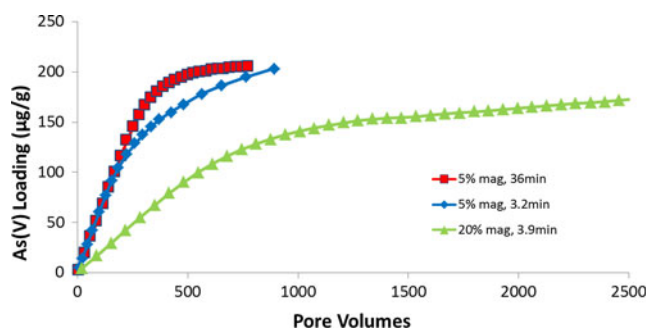


**FIG. 4.** Cumulative mass of As(V) adsorbed per gram of nanomagnetite contained within each column. Solid lines are for visualization only.

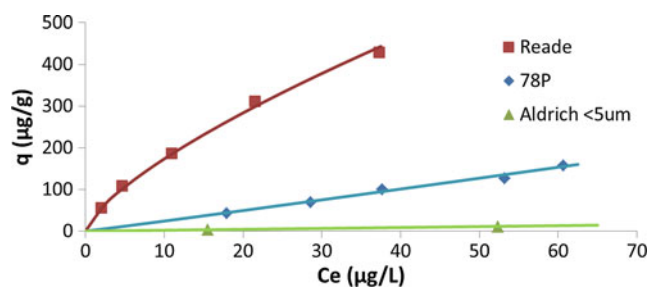


**FIG. 5.** As(V) adsorption isotherms for commercial magnetite particles in Evangeline groundwater. Solid lines display the least squares curve fit to Freundlich isotherms.

due to mechanical transport effects such as preferential flow away from larger aggregates of fine magnetite particles with low permeability and increased surface to surface contact of magnetite that may limit access to adsorption sites.

Figure 4 shows that for the two columns with similar residence time, less arsenic adsorbed per gram in the 20% column (175  $\mu\text{g/g}$ ) by 2,500 PV than adsorbed in the 5% column (205  $\mu\text{g/g}$ ) by termination of the experiment at 900 PV. Essentially, a slower approach to maximum adsorption capacity is observed when more magnetite is in the column. Furthermore, the maximum adsorption capacity observed for the magnetite in the columns was 40–50% below that determined from batch adsorption isotherms. In a 24-h adsorption isotherm (not shown) conducted with magnetite mixed in the same groundwater and equilibrium concentration (100  $\mu\text{g/L}$ ), 349  $\mu\text{g}$  of arsenic adsorbed to each gram of magnetite. The reduced adsorption capacity observed in the column systems may be due to preferential flow paths, inaccessible surface sites, and adsorption and interaction of competing species continuously introduced with the feed solution (Konikow, 2010).

When the flow rate for a 5% by weight nanomagnetite column was regulated to yield a 36 min residence time, initial breakthrough ( $C/C_0=0.10$ ) was delayed by a factor of 1.9 on a PV basis than the identically packed column (5% by weight nanomagnetite) with a 3.2 min residence time. Although initial breakthrough was delayed, the point of 90% break-

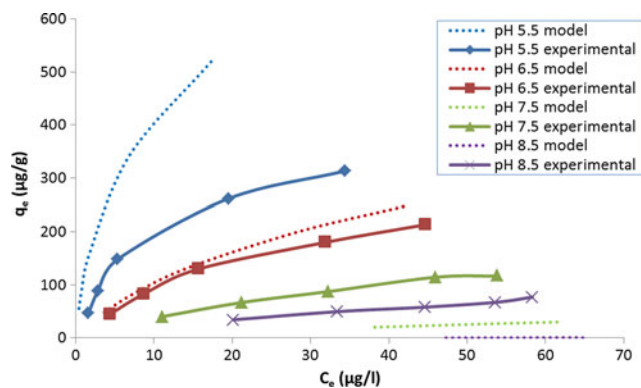


**FIG. 6.** pH influence on 24-h isotherms (modeled by Visual Minteq and experimental) for arsenic adsorption to 78P magnetite in As(V)-spiked Guanajuato groundwater. Solid lines are for visual aid only.

through ( $C/C_0=0.90$ ) was obtained at an earlier PV than for the 3.2 min residence time column (Fig. 3). The 36 min residence time more efficiently removes arsenic and presumably other competing species at earlier PVs, but then adsorption sites are less available at later PVs than for the shorter 3.2 min residence time operation. The arsenic being removed more efficiently at early PVs was offset by the less removed at later PVs to yield about same cumulative total of arsenic removed by 800–900 PV (Fig. 4).

In summary, these column studies suggest that by adjusting the hydraulic residence time and magnetite-to-sand ratio, controlled arsenic elution profiles could be obtained accordingly for a particular application. For point-of-use applications (e.g., household biosand filters in developing nations) where less treated water is needed but extended operation before initial breakthrough is critical, a single filter with a residence time of 36 min or longer and a high ratio of magnetite to sand would be suggested to delay initial breakthrough. Alternatively, for large-scale systems, where maximum throughput is desired, short residence times could be used with modular columns in series. This would allow the full capacity of the initial column to be exhausted while columns downstream would ensure an effluent quality with near nondetectable levels of arsenic. At exhaustion, the initial column could be taken offline for regeneration and put back in service as the final column in the treatment train, and so forth. Although lowering the magnetite to sand ratio below 20:80 would yield more efficient columns on a per mass of magnetite basis, it also would decrease the column capacity thus shortening the time between regenerations. Ultimately, the appropriate ratio of magnetite to sand would be driven by system economics.

#### Magnetite selection for field column

A selection of magnetite products were assessed based on mass of arsenic adsorbed per gram of solid ( $q_e$ ), product safety considerations, and cost to determine suitability for further laboratory and field-study experiments. The As(V) adsorption isotherms are shown in Figure 5 for two nano-sized iron oxides and, for reference, 1  $\mu\text{m}$ -sized iron oxide (<5  $\mu\text{m}$ ; Sigma-Aldrich). Other less effective materials were omitted for figure clarity. Although Reade nanomagnetite was the most effective, the 78P nanomagnetite marketed by a pigment manufacturer, Rockwood Pigments, was selected for the field study based on cost considerations and given its food-grade certification. A summary of physical, adsorption, and economic considerations is summarized in Table 2.

The treatment cost (far right column) in Table 2 is based on adsorption isotherm data for the given conditions and does not take into account how (1) interfering species may affect column systems differently than in batch isotherms, (2) mass transfer kinetics may not scale proportionally from batch to full-scale, (3) regeneration may affect subsequent adsorption cycles, (4) fluctuations in inlet water chemistry such as inlet arsenic concentration, pH, temperature, and other seasonal variations, may affect removal, and (5) pressure build-up may occur more readily in full-scale columns and require back-wash cycles that perturb the mass-transfer zone within a column. Therefore, several simplifying assumptions were made for the cost analysis: (1) Given kinetic and preloading limitations, the each column media was taken to adsorb a set

TABLE 2. PRODUCT COMPARISON AND ADSORBENT COST PROJECTIONS FOR A SELECTION OF MAGNETITE PRODUCTS

Adsorbent	Food grade	Bulkcost \$/kg	SSA m <sup>2</sup> /g	K <sub>F</sub> μg/g · (L/μg) <sup>1/n</sup>	1/n	R <sup>2</sup>	q <sub>e</sub> μg/g	q <sub>e</sub> μg/m <sup>2</sup>	Treatment cost \$/m <sup>3</sup>
Reade n-mag	No	260	60	33.8	0.71	1.00	380	6.33	1.52
Rockwood 78P	Yes	5.5	12	2.26	1.03	0.99	74.5	6.15	0.16
Sigma-Aldrich < 5 μm	No	2.2	—				6.53		0.75

fraction (0.75 assumed in Table 2) of the concentration predicted by the 24-h adsorption isotherm. (2) Feed water with a constant 30 μg/L As(V) would be treated by columns arranged in series and blended with raw water to a target concentration of 25 μg/L, the Mexican drinking water standard. (3) Only adsorption of As(V) was considered, although As(III) has been shown to adsorb with similar affinity to magnetite nanoparticles (Shipley, 2007). Furthermore, from the redox potential (200 mV) and dissolved oxygen concentration (3.2 mg/L) in the Guanajuato groundwater measured directly at the well, arsenic should predominantly be in the As(V) form. (4) Regeneration cycles (two in this case) were assumed to recover all adsorbed arsenic, returning media to its virgin state for subsequent adsorption steps. Although regeneration of arsenic from magnetite adsorbents must be further studied, arsenic desorption from one hydrous ferric oxide (HFO) media has been reported to be carried out with four bed volumes of a 10% NaOH solution with an empty bed contact time of 6 min (Sylvester *et al.*, 2007). The regenerated media showed improved adsorption capacity over the virgin media. (5) Costs for auxiliary materials, construction, labor, operation, regeneration, and disposal were not considered.

Adsorbent cost, in dollars per cubic meter of treated water, is calculated based on the equation below. For the assumptions stated, it is important to note that the lowest cost adsorbent by this calculation may not result in the most economical treatment process (Chen *et al.*, 1999).

$$\text{Cost} \left[ \frac{\$}{\text{m}^3} \right] = \frac{\text{Media Cost} \left[ \frac{\$}{\text{kg}} \right]}{q_e \left[ \frac{\mu\text{g}}{\text{g}} \right] \times \text{Fraction of Isotherm} \times 1000 \left[ \frac{\text{g}}{\text{kg}} \right]} \times \left( C_{\text{As, initial}} \left[ \frac{\mu\text{g}}{\text{L}} \right] - C_{\text{As, target}} \left[ \frac{\mu\text{g}}{\text{L}} \right] \right) \times 1000 \left[ \frac{\text{L}}{\text{m}^3} \right] \div (1 + \text{No. of Regeneration Cycles})$$

The 78P magnetite resulted in an estimated cost of \$0.16/1,000 L when treated water is blended with raw water to comply with the Mexican contaminant limit and regeneration is taken into account. The treatment cost was ~5 times less than micron-sized magnetite from Sigma-Aldrich and 10 times less than Reade nanomagnetite.

#### pH-dependent batch isotherms

Adsorption isotherms were developed using pH-adjusted Guanajuato groundwater and modeled with corresponding solution conditions in Visual Minteq (Fig. 6). Given the large body of equilibrium data available from Dzombak and Morel (1990) for HFO and based on previous experience with nanomagnetite point-of-zero-charge (pzc) and adsorption, an assumption was made that arsenic adsorption and changes in

adsorption due to changes in solution parameters would be similar to that of HFO when normalized by surface area (Yavuz *et al.*, 2006; Yean, 2008). Although the modeling over-predicted the effect of pH, both data sources were in agreement that pH reduction would significantly increase the amount of arsenic adsorbed to magnetite. For an aqueous arsenic concentration of 16 μg/L, the inlet concentration of pH-adjusted field column experiments, the experimentally measured K<sub>d</sub> values (determined using the highest solution/solid concentrations) at pH 8.5, 7.5, 6.5, and 5.5 were 1.8, 3.3, 8.3, and 15 L/g, respectively. The deviation of model predictions from experimental data may be due to ability of the surface complexation modeling to account for the simultaneous interactions of all species in solution. The increase in arsenic adsorption at low pH was attributed to the more positive magnetite surface charge with decreasing pH. Above the p<sub>H<sub>pzc</sub></sub> of magnetite (6.8), the negatively charged surface repels arsenate anions (Yean, 2008). The repulsive force is amplified as the predominant arsenate species changes from H<sub>2</sub>AsO<sub>4</sub><sup>-</sup> to HAsO<sub>4</sub><sup>2-</sup> as pH rises above the pK<sub>a2</sub> of 6.94. As pH is further increased, if silica species are present in solution, a small fraction of the adsorbed silicates adopt a negative charge in relation to the pK<sub>a1</sub> of silicic acid (9.46), causing further repulsion of arsenate. Both the modeled and the experimental isotherms shift from Freundlich behavior (curved) to linear as the pH increases. At low pH, adsorption of the arsenate species adsorbs so significantly that the surface charge on the magnetite becomes more negative as the arsenic concentration in the system increases. At higher adsorbed concentrations, the electrostatic interaction becomes less favorable, which results in the observed curve in the adsorption isotherm. This effect is less significant at pH conditions above the p<sub>H<sub>pzc</sub></sub> because the concentration of arsenic on the solid is sufficiently low.

In addition, a batch adsorption isotherm was conducted by hot water bath at the temperature of Guanajuato well No. 8 (40°C) and in oxygen-deficient conditions, but essentially no change in adsorption behavior was observed compared to the isotherms conducted at room temperature and exposed to the atmosphere.

#### Field columns

In contrast to the modeled and observed effect on batch isotherm experiments, pH reduction did not improve arsenic adsorption in column experiments conducted in the field with Guanajuato groundwater (Fig. 7). Pilot-scale columns were constructed in Guanajuato to test arsenic breakthrough with raw and pH-adjusted groundwater. Approximately 5,000 L of groundwater were passed through each column at 1 L/min over the course of 3–4 days with a residence time of 0.75 min. The flow rate was selected to give a realistic flux in relation to industrial rapid sand filters, a potential target application for

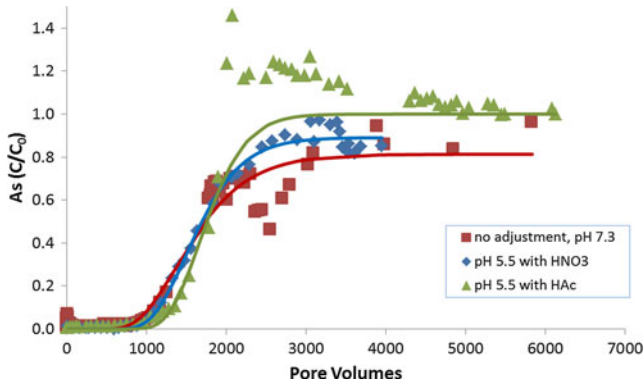


**FIG. 7.** Arsenic breakthrough with untreated and pH-adjusted groundwater by  $\text{HNO}_3$  and acetic acid (HAc) in Guanajuato groundwater passed through the pilot column.  $[\text{As}]_{\text{inlet}} = 7.8 \mu\text{g/L}$  for raw groundwater and  $16 \mu\text{g/L}$  for pH-adjusted experiments. Solids lines are fitted by CXTFIT.

Guanajuato. The flow resulted in a flux of  $7.5 \text{ m}^3/[\text{h} \cdot \text{m}^2]$ , 15% below the maximum recommended flux rate for rapid sand filters (Ives, 1985). For other applications such as slow sand filtration, a reduced flux and increased residence time could be used to yield an improved breakthrough profile. The column fed with raw groundwater (Fig. 7, pH 7.3) removed 99% of the influent arsenic for  $\sim 1,000$  PV before initial breakthrough. By numeric integration between the influent and effluent concentration curves over the entire experiment, magnetite in the column had adsorbed, on average,  $20.3 \mu\text{g}$  of arsenic per gram of magnetite. Given a final influent concentration of  $6.8 \mu\text{g/L}$  of arsenic, this corresponded to a  $K_d$  of  $3.0 \text{ L/g}$ . This is equivalent to saying that the magnetite within the column adsorbed, on average, the equivalent arsenic contained in  $3.0 \text{ L}$  of the feed solution. It was observed that the arsenic breakthrough remained constant between  $1,900$  and  $2,400$  PV and then dropped significantly at  $\sim 2,400$  PV. Beyond  $2,500$  PV the effluent concentration steadily increased and trended toward convergence with the influent concentration with some oscillation. The drop at  $2,400$  PV may have been correlated to surface oxidation of magnetite within the column. Although not directly evaluated, at the given pH (7.3) and redox potential (237 mV) conditions, the magnetite surfaces were not thermodynamically stable and could have slowly oxidized to ferric hydroxide over time. The corrosion products may, in fact, adsorb arsenic more strongly than magnetite (Ngai *et al.*, 2007). Furthermore, additional surface area for adsorption would be created by corrosion products, especially if cleaved. Any cleaved corrosion fines would have likely been retained by the supporting sand layer of the column. By total iron analysis of unfiltered samples, no corrosion fines were detected in the column effluent water.

The effects of iron were most certainly a factor in the raw groundwater pilot experiment, as the metal pipe released red rust during an initial flush of the piping system before the column experiment. The pipes were flushed for several hours before starting the experiment; however, the arsenic concentration in the inlet water just before the column was only  $5\text{--}6 \mu\text{g/L}$  by the beginning of the experiment as compared to  $9.7 \mu\text{g/L}$  in the water truck feed tank. The inlet arsenic concentration rose from  $5$  to  $7 \mu\text{g/L}$  by the end of the experiment. For the other pilot-column experiments, clean PVC lines

were installed to connect the water truck feed tank to the column to prevent contact with oxidized iron in the conveyance system.

Acetic acid was used for its self-buffering capacity to adjust the pH of another water truck feed tank to the desired level of 5.5; however, after observing no significant improvement in breakthrough from the raw groundwater case and considering that acetate ion may compete for adsorption sites, nitric acid was used to condition another feed tank to pH 5.5. Figure 7 shows that both the pH-adjusted feed solutions were ineffective in significantly improving arsenic adsorption from the raw groundwater experiment. Initial breakthrough was similar for all three columns, each occurring near  $1,000$  PV. For the feed tank adjusted with acetic acid, the effluent arsenic concentration rose to over 140% breakthrough after  $2,000$  PV of treated water. There might be several explanations for this rise above  $C/C_0 > 1$ . Changes in redox of the iron surface species could have released arsenic from the adsorbed phase. Another explanation might be related to competition between the acetate and arsenate anions.

The final  $K_d$  obtained for the acetic acid adjusted experiment rose to a maxima of  $2.6 \text{ L/g}$  before dropping to  $1.9 \text{ L/g}$  by the end of the experiment. The  $K_d$  for the nitric acid adjusted experiment reached  $3.1 \text{ L/g}$  by the end of the experiment. These are similar to the  $K_d$  of  $3.0 \text{ L/g}$  obtained in the raw groundwater experiment. The pH adjustment did not have a discernible impact on the total quantity of arsenic removed by the columns. Given the  $K_d$  of  $3.0 \text{ L/g}$  and the  $456 \text{ g}$  (ca.  $\$2.5$  USD) of magnetite present in the column, the column effectively removed the equivalent mass of arsenic contained in  $1,368 \text{ L}$  of Guanajuato groundwater. In a process scenario, the arsenic-free water could then be blended back with untreated water to an arsenic concentration within the contaminant limit to reduce throughput requirements and treatment costs.

In contrast to batch isotherms, which improved significantly with a reduction in pH, column experiments showed almost no removal improvement. This difference may have been due to preloading of competitive species, redox processes involving iron, or short residence times in the field columns as compared to any previous experiments. Considering the same aqueous-phase arsenic concentration, the pH 7.5 isotherm experiment (Fig. 6) yielded a similar  $K_d$  ( $2.9 \text{ L/g}$ ) to that calculated from the pilot-column experiment at pH 7.3 ( $3.0 \text{ L/g}$ ), while at pH 5.5 the isotherm experiment adjusted by  $\text{HNO}_3$  was much higher ( $10 \text{ L/g}$ ) than the corresponding pilot-column experiment adjusted by  $\text{HNO}_3$  ( $3.1 \text{ L/g}$ ). Preloading may be a significant contributor to the lack of improvement in arsenic removal for the column studies with pH reduction. Preloading occurs when arsenic is retained in early portions of the column, while lesser-retained species, pass through and interact with the later portions of the column. Lesser retained species could be any constituent present in high concentrations (e.g.,  $> 1 \text{ mg/L}$ ) that has relatively rapid breakthrough, such as silica, sulfate, or phosphates. Pre-exposure to these constituents may foul adsorbent media, reducing capacity for arsenic adsorption, and accelerate the breakthrough of arsenic. It has been postulated that fouling occurs by reorientation of the fouling species on the adsorbent surface over time, potentially by polymerization (Knappe *et al.*, 1997). For example, as silica transitions from monodentate mononuclear to bidentate binuclear attachment,



its adsorption becomes irreversible. Silica was suspected as an interfering species as its concentration is very high in the Mexico groundwater (48 mg/L as SiO<sub>2</sub>) and it experienced immediate breakthrough in the column studies. Given this, the magnetite toward the outlet of the column would show a reduced capacity for arsenic than magnetite at the inlet of the column, which is a topic of future work. Other factors contributing to the difference between column and batch results may include ion exchange of arsenic already adsorbed to the surface with competing species, kinetic-limited operation of the column, and nonideal flow paths. Improvement to the overall system should focus on increasing the surface area of magnetite within a given reactor volume and mitigating the effects of competing species.

No adverse effects to the groundwater were observed as a result of treatment by the nanomagnetite-enhanced sand columns. In each column during packing of the sand/nano-magnetite mixture and initial startup, there was a small (ca. 1 cm) transition zone that developed in which some black nanomagnetite aggregates migrated and darkened the adjacent sand. However, any migration was contained to this transition zone, which remained static over the course of each experiment. Water samples collected from the column did not show any breakthrough of nanomagnetite, neither visually nor by measurement of total iron. Further, upon implementation, a magnet positioned at the treatment outlet could be used for an added safety measure to ensure no breakthrough of magnetite. Furthermore, after arsenic removal, the quality of the treated water was within the WHO (2011) guidelines for drinking water quality in regard to the applicable elements measured by ICP-OES and ICP-MS (As, Cr, Cu, Pb, Se, and U).

## Summary

Guanajuato city officials and CBEN researchers at Rice University collaborated to bring previous laboratory work with nanomagnetite, as an arsenic adsorbent technology, to a demonstration level with pilot columns. First, nanomagnetite (20 and 100 nm) was used in batch isotherm and column studies to determine column design and operating conditions and to estimate arsenic treatment costs. During the accompanying pilot study in Guanajuato, the equivalent quantity of arsenic contained in 1,360 L of well water was removed using 456 g of economically viable, food-grade nanoparticulate magnetite pigment (78P; Rockwood Pigments). The mass ratio of magnetite to sand within a column was determined to be the most important factor affecting arsenic removed. Although the shape of the breakthrough curve was altered by residence time, the final arsenic adsorbed per mass of magnetite in the column was eventually the same for columns with similar mass of magnetite. Therefore, packed filters with short residence times in series may be ideal for treating large quantities of water under similar conditions. Reducing pH from 7.3 to 5.5 did not improve column breakthrough (i.e., material sorption efficiencies) for Guanajuato groundwater, despite improvement in batch adsorption isotherms. Other chemical phenomena occurring in columns not present in adsorption isotherms (kinetic effects, increased adsorption of interferences, and surface changes) are possible explanations. A future study with household-scale sand filters where intermittent and reduced flow would minimize kinetic effects

and prolong filter life may yield promising results. Further, regeneration of the magnetite media and mitigation of competing species may multiply filter life by a significant factor. Beyond sand, other media may be more ideal to support and evenly disperse a greater mass of magnetite within a column for longer filter life.

This work incorporates one of the most well-studied nanoscale iron oxides, nanomagnetite, into one of the most basic water treatment processes, sand-filtration, for arsenic removal in field application. This offers potential benefits for point-of-use household treatment or cities with much lower technical support than major U.S. cities, but these benefits will only be realized after extensive testing with realistic water samples and conditions.

## Acknowledgments

This research was supported by the Rice University Center for Biological and Environmental Nanotechnology (CBEN), which was funded in part through the Nanoscale Science and Engineering Initiative of the National Science Foundation under NSF Award Number EEC-0118007 and EEC-0647452.

## Author Disclosure Statement

No competing financial interests exist.

## References

- Anderson, M.A., Ferguson, J.F., and Gavis, J. (1976). Arsenate adsorption on amorphous aluminum hydroxide. *J. Colloid Interface Sci.* 54, 3.
- Arai, Y., and Sparks, D.L. (2002). Residence Time Effects on Arsenate Surface Speciation at the Aluminum Oxide-Water Interface. *Soil Sci.* 167, 5.
- Bujnakova, Z., Balaz, P., Zorkovska, A., Sayagues, M.J., Kovac, J., and Timko, M. (2013). Arsenic sorption by nanocrystalline magnetite: an example of environmentally promising interface with geosphere. *J. Hazard. Mater.* 262, 1204.
- Chen, H.W., Frey, M.M., Clifford, D., McNeill, L.S., and Edwards, M. (1999). Arsenic treatment considerations. *J. Am. Water Works Assoc.* 91, 74.
- Chowdhury, S.R., Yanful, E.K., and Pratt, A.R. (2011). Arsenic removal from aqueous solutions by mixed magnetite-maghemite nanoparticles. *Environ. Earth Sci.* 64, 411.
- Dixit, S., and Hering, J.G. (2003). Comparison of Arsenic(V) and Arsenic(III) Sorption onto Iron Oxide Minerals: Implications for Arsenic Mobility. *Environ. Sci. Technol.* 37, 18.
- Dzombak, D.A., and Morel, F.M.M. (1990). *Surface Complexation Modeling: Hydrous Ferric Oxide*. New York: Wiley-Interscience.
- Gimenez, J., Martinez, M., de Pablo, J., Rovira, M., and Duro, L. (2007). Arsenic sorption onto natural hematite, magnetite, and goethite. *J. Hazard. Mater.* 141, 575.
- Gupta, S.K., and Chen, K.Y. (1978). Arsenic Removal by Adsorption. *J. Water Pollution Control Federation.* 50, 3.
- Gustafsson, J.P. (2012). *Visual MINTEQ v3.0*. Stockholm: KTH Royal Institute of Technology, Dept. of Land and Water Resources Engineering.
- Hingston, F.J., Posner, A.M., and Quirk, J.P. (1971). Competitive adsorption of negatively charged ligands on oxide surfaces. *Disc. Faraday Soc.* 52, 334.

- Hristovski, K., Baumgardner, A., and Westerhoff, P. (2007). Selecting metal oxide nanomaterials for arsenic removal in fixed bed columns: from nanopowders to aggregated nanoparticle media. *J. Hazard. Mater.* 147, 265.
- Huang, C.P., and Fu, L.K. (1984). Treatment of arsenic(V)-containing water by activated carbon. *J. Water Pollut. Control Fed.* 56, 233.
- Ives, K.J. (1985). *Deep Bed Filters*. Dordrecht: Martinus Nijhoff Publishers.
- Jonsson, J., and Sherman, D.M. (2008). Sorption of As(III) and As(V) to siderite, green rust (fougerite) and magnetite: implications for arsenic release in anoxic groundwaters. *Chem. Geol.* 255, 173.
- Knappe, D.R.U., Snoeyink, V.L., Roche, P., Prados, M.J., and Bourbigot, M.M. (1997). The effect of preloading on rapid small-scale column test predictions of atrazine removal by GAC adsorbents. *Water Res.* 31, 2899.
- Konikow, L. (2010). The secret to successful solute-transport modeling. *Ground Water* 49, 144.
- Mamindy-Pajany, Y., Hurel, C., Marmier, N., and Romeo, M. (2011). Arsenic (V) adsorption from aqueous solution onto goethite, hematite, magnetite and zero-valent iron: effects of pH, concentration and reversibility. *Desalination* 281, 93.
- Mayo, J.T., Yavuz, C., Yean, S., Cong, L., Shipley, H., Yu, W., Falkner, J., Kan, A., Tomson, M., and Colvin, V. L. (2007). The effect of nanocrystalline magnetite size on arsenic removal. *Sci. Technol. Adv. Mater.* 8, 71.
- Mohan, D., and Pittman, C.U. Jr. (2007). Arsenic removal from water/wastewater using adsorbents—A critical review. *J. Hazard. Mater.* 142, 1.
- Navas-Acien, A., Silbergeld, E.K., Pastor-Barriuso, R., and Guallar, E. (2008). Arsenic exposure and prevalence of type 2 diabetes in US adults. *J. Am. Med. Assoc.* 300, 814.
- Ngai, T.K., Shrestha, R.R., Dangol, B., Maharjan, M., and Murcott, S.E. (2007). Design for sustainable development—household drinking water filter for arsenic and pathogen treatment in Nepal. *J. Environ. Sci. Health A Tox. Hazard. Subst. Environ. Eng.* 42, 1879.
- Phillips, M., and Salmeron, J. (1992). Diabetes in Mexico—a serious and growing problem. *World Health Stat. Q* 45, 338.
- Plant, J.A., Kinniburgh, D.G., Smedley, P.L., Fordyce, F.M., and Klinck, B.A. (2005). *Arsenic and Selenium*. Amsterdam: Elsevier Science.
- Raven, K.P., Jain, A., and Loeppert, R. H. (1998). Arsenite and Arsenate Adsorption on Ferrihydrite: Kinetics, Equilibrium, and Adsorption Envelopes. *Environ. Sci. Technol.* 32, 344.
- Septien, J.M.V., Ojeda, L.M. (1983). El agua en la ciudad de Guanajuato, problema de siglos. Secretaria de Programacion del Estado de Guanajuato, 84 pages.
- Shipley, H.J. (2007). *Magnetite Nanoparticles for Removal of Arsenic from Drinking Water*. Dissertation. Houston: Rice University.
- Shipley, H.J., Yean, S., Kan, A.T., and Tomson, M.B. (2009). Adsorption of arsenic to magnetite nanoparticles: effect of particle concentration, Ph, ionic strength, and temperature. *Environ. Toxicol. Chem.* 28, 509.
- Sylvester, P., Westerhoff, P., Moller, T., Badruzzaman, M., and Boyd, O. (2007). A hybrid sorbent utilizing nanoparticles of hydrous iron oxide for arsenic removal from drinking water. *Environ. Eng. Sci.* 24, 104.
- Toride N., Lejj, F.J., and van Genuchten, M.Th. (1995). The CXTFIT Code for Estimating Transport Parameters from Laboratory or Field Tracer Experiments. v2.0. U.S. Salinity Laboratory Agricultural Research Service, Riverside, CA. Rep. 137.
- Wang, L., and Chen, A.S.C. (2011). *Costs of Arsenic Removal Technologies for Small Water Systems: U.S. EPA Arsenic Removal Technology Demonstration Program T. J. Sorg.* Cincinnati: United States Environmental Protection Agency, p. 92.
- World Health Organization (WHO) (2011). *Guidelines for Drinking-Water Quality*. 4th Edn. Malta: World Health Organization.
- Yavuz, C.T., Mayo, J.T., Yu, W.W., Prakash, A., Falkner, J.C., Yean, S., Cong, L., Shipley, H.J., Kan, A., Tomson, M., Natelson, D., and Colvin, V.L. (2006). Low-field magnetic separation of monodisperse Fe<sub>3</sub>O<sub>4</sub> nanocrystals. *Science* 314, 964.
- Yean, S.J. (2008). Arsenic Removal Using Iron Oxides: Application of Magnetite Nanoparticles and Iron Salts. Doctor of Philosophy, Rice University.